Steel and Composite Structures, *Vol. 21*, *No. 2* (*2016*) *373-394*
DOI: http://dx.doi.org/10.12989/scs.2016.21.2.373

Postbuckling analysis of laminated composite shells under shear loads

Woo-Young Jung [1], Sung-Cheon Han [2], Won-Hong Lee [3**] and Weon-Tae Park [*4]

[1] *Department of Civil Engineering, Gangneung-Wonju National University, 7 Jukheon, Gangneung, 210-702, Republic of Korea*
[2] *Department of Civil & Railroad Engineering, Daewon University College, 599 Shinwol, Jecheon, 390-702, Republic of Korea*
[3] *Department of Civil Engineering, Gyeongnam National University of Science and Technology, 33 Dongjin, Jinju, 660-758, Republic of Korea*
[4] *Division of Construction and Environmental Engineering, Kongju National University, 275 Budai, Cheonan, 330-717, Republic of Korea*

(*Received February 23, 2015, Revised March 29, 2016, Accepted April 07, 2016*)

Abstract. The postbuckling behavior of laminated composite plates and shells, subjected to various shear loadings, is presented, using a modified 8-ANS method. The finite element, based on a modified first-order shear deformation theory, is further improved by the combined use of assumed natural strain method. We analyze the influence of the shell element with the various location and number of enhanced membrane and shear interpolation. Using the assumed natural strain method with proper interpolation functions, the present shell element generates neither membrane nor shear locking behavior even when full integration is used in the formulation. The effects of various types of lay-ups, materials and number of layers on initial buckling and postbuckling response of the laminated composite plates and shells for various shear loading have been discussed. In addition, the effect of direction of shear load on the postbuckling behavior is studied. Numerical results and comparisons of the present results with those found in the literature for typical benchmark problems involving symmetric cross-ply laminated composites are found to be excellent and show the validity of the developed finite element model. The study is relevant to the simulation of barrels, pipes, wing surfaces, aircrafts, rockets and missile structures subjected to intense complex loading.

Keywords: laminated composite shells; postbuckling analysis; assumed natural strain; shear loads

1. Introduction

Laminated composite plates and shells are one of the major load bearing elements in aerospace, civil, underwater, nuclear reactors and other important high-performance engineering structures due to their high specific strength and high specific stiffness. These elements are subjected to severe and varying loading directions during their service life leading to failure due to large amounts of deflection or excessive stresses. They are now used for many primary load carrying structures such as aircrafts, rockets, wing surfaces, barrels, cylinders and missile skins. Plates and

∗Corresponding author, Professor, E-mail: pwtae@kongju.ac.kr
** Professor, E-mail: whyee@gntech.ac.kr

http://www.techno-press.org/?journal=scs&subpage=6 ISSN: 1229-9367 (Print), 1598-6233 (Online)

shells made of laminated composite of fiber reinforced plastics are probably the most important structural members. Draiche *et al*. (2014) studied a vibration analysis of laminated composite plates using the refined plate theory. To exploit the efficiency of these materials with high performance and high cost, scientists and engineers have made continuous efforts to develop analytical, numerical and experimental techniques to reveal and to predict the buckling and postbuckling behavior of such plates and shells.

The effect of transverse shear deformation on buckling behavior of symmetrically laminated plates was investigated by Whitney (1969a, b) and Vinson and Chou (1975). They showed that transverse shear deformation can be significant, not only in altering the magnitudes of the buckling loads, but also in changing their mode shapes when the ratio of thickness to the other dimensions is relatively large. Reddy (1984) proposed a higher order theory. Reddy and his co-researchers studied the initial buckling of laminated composite plates using this higher order shear deformation theory. Tanov and Tabiei (2000) presented approach for treating the transverse shear strains and stresses in homogeneous shells results in parabolic distribution for both strains and stresses and, therefore, it eliminates the need of any shear correction factors. Considering that only the higher-order terms in the transverse shear strains expressions is presented, Tanov and Tabiei (2000) assumption does not preserve the efficiency of first-order shear deformation theory perfectly. Recently, in space industries advanced composite materials such as functionally graded materials are employed and some advanced four and five higher order theories are developed by many researchers (Tounsi *et al*. 2013, Bachir Bouiadjr *et al*. 2013, Bouderba *et al*. 2013, Hebali *et al*. 2014, Belabed *et al*. 2014, Ait Amar Meziane *et al*. 2014, Zidi *et al*. 2014, Bousahla *et al*. 2014, Han *et al*. 2015, Hamidi *et al*. 2015, Bourada *et al*. 2015, Ait Yahia *et al*. 2015, Mahi *et al*. 2015, Bennoun *et al*. 2016).

Buckling and post-buckling characteristics are one of the major design criteria for laminated composite plates and shells for their optimal usage. Hence, it is important to study the buckling and post-buckling characteristics of laminated composite plates and shells under various loadings for accurate and reliable design. The buckling of rectangular laminated composite plates has been the subject of study for many investigators during the past. A great deal of initial buckling analyses for plates with various lay-ups, different loading, boundary and geometry conditions may be found in the literature. Jones (1973) used exact solutions to study the buckling of rectangular plates with unsymmetrical cross-ply and angle-ply lay-up. His results show that the effects of unsymmetrical laminating can be more severe in reducing the buckling load than exists for the anti-symmetric case. However, limited investigations on the postbuckling behavior of laminated composite plates and shells under the shear loads are previously conducted.

Early investigations related to shear buckling and postbuckling response of laminated plates are the works of Zhang and Matthews (1983a, b) and Kosteletos (1992). Both analytical and experimental studies for cylindrically curved panels of laminated composite materials are far fewer that for flat plates. Kudva (1979) presented a finite element analysis for the investigation of the postbuckling behavior of symmetrically laminated curved panels. Only a few examples were computed and the effects of boundary conditions, loading conditions, geometry conditions and stretching-bending coupling on the postbucking behavior were not considered. The research for buckling of laminated curved panels under shear loading was performed by Wilkins and Olson (1974).

Balamurugan *et al*. (1998) studied postbuckling behavior of laminated composite plates under in-plane shear loads using a 9-node shear flexible quadrilateral plate element. Kim *et al*. (2003) carried out initial buckling and postbuckling analysis of composite plates under pure shear loading.

cKumar and Singh (2010) presented the postbuckling strength of composite laminates with cutouts under in-plane shear. In 2014, Gupta *et al*. (2014) investigated postbuckling response and progressive failure of composite laminated plates considering geometric nonlinearity and evolving material damage under in-plane shear loadings. It should be noted that they only investigated postbuckling behavior of laminated composite plates. Taken as a whole, very few studies were conducted on the postbuckling analysis of the laminated composite shells under the in-plane shear loading. Thus, needs exist for the development of shell finite element which is simple to use for postbuckling analysis of laminated composite shells.

The work of Huang and Hinton (1986) in which, unfortunately, the 8-node element passed the relevant tests described in the paper but gives less accurate results than the 9-node quadrilateral element. Lakshminarayana and Kailash (1989) presented an 8-node shell element which is free of locking. In order to resolve the locking problem, they used appropriately chosen interpolation functions based on Hinton and Huang's concept. Bucalem and Bathe (1993) have improved previous studies on the MITC8 shell elements (1986) and concluded that while it performed quite effectively in some cases, in a few analyses the element presented a very stiff behavior, which showed it was not useful and desirable to be improved. Kim *et al*. (2003) presented an 8-node shell finite element. In their study, to eliminate both the shear locking and membrane locking, the assumed strain method developed by Ma and Kanok-Nukulchai (1989) was applied to the natural coordinate. However, the persistence of locking problems was observed throughout the numerical experiments for 8-node shell element on standard test problems of MacNeal and Harder (1985). In order to improve the 8-node ANS shell element, a new combination of sampling points is adopted for postbuckling analysis of laminated composite shells.

In this paper, we concentrate on the postbuckling analysis of laminated composite shells under the in-plane shear loading, using the curved quadrilateral shell finite element, which can be viewed as the 8-node element from a practical point of view. For a composite laminate, the shear direction, the orientation of fiber angle and layup sequences could play a dominant role in determining the nonlinear characteristics. Thus, current study is further extended to take into account the effects of shear loading and stacking sequences. This study use the modified first-order shear deformation theory and verify the numerical results by comparing the results with the analytical solutions obtained by Zhang and Matthews (1985).

2. Modified first-order shear deformation theory

In Fig. 1, the geometry of an 8-noded shell element with six degrees of freedom is shown.

The higher-order shear deformation theory to be adopted in this study is based on the assumption for degenerated shell element that the originally straight normal to the mid-surface can deform into a cubic-order function with respect to the thickness coordinate. The displacement field of the third-order shear deformation theory of shells is given by (For more details, see Jung and Han (2014))

$$\mathbf{P}(\xi_i) = \overline{\mathbf{P}}(\xi_j) + \xi_3\,\overline{\mathbf{V}}(\xi_j) + \xi_3^3\boldsymbol{\Psi}(\xi_j) = \overline{\mathbf{P}}(\xi_j) + \xi_3\left(1-\frac{\xi_3^2}{3}\right)\overline{\mathbf{V}}(\xi_j) \tag{1}$$

$$\mathbf{u}(\xi_i) = \overline{\mathbf{u}}(\xi_j) + \xi_3\,\overline{\mathbf{e}}(\xi_j) + \xi_3^3\boldsymbol{\psi}(\xi_j) = \overline{\mathbf{u}}(\xi_j) + \xi_3\left(1-\frac{\xi_3^2}{3}\right)\overline{\mathbf{e}}(\xi_j) \tag{2}$$

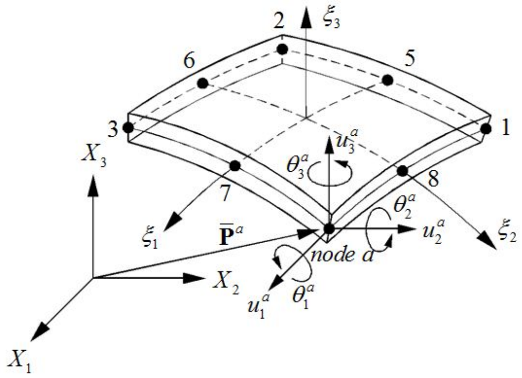

Fig. 1 Geometry of 8-node shell element with six degrees of freedom

where $\mathbf{P}$ denotes the position vector of a generic point in the shell element; $\overline{\mathbf{P}}$ and $\overline{\mathbf{V}}$ are the position vector of a point in the mid-surface and a normal vector to the mid-surface, respectively; $\overline{\mathbf{u}}$ and $\overline{\mathbf{e}}$ are the translational displacement vector and the fiber displacement vector of a point in the mid-surface, respectively.

By substituting Eqs. (1) and (2) into the tensor transformation relationship of Green strain tensor and the natural strain, the strains and transverse natural shear strains can obtain

$$\widetilde{E}_{\alpha\beta} = \frac{1}{2}\left[\frac{\partial \mathbf{P}_I}{\partial \xi_\alpha}\frac{\partial \mathbf{u}_I}{\partial \xi_\beta} + \frac{\partial \mathbf{u}_J}{\partial \xi_\alpha}\frac{\partial \mathbf{P}_J}{\partial \xi_\beta} + \frac{\partial \mathbf{u}_K}{\partial \xi_\alpha}\frac{\partial \mathbf{u}_K}{\partial \xi_\beta}\right] \tag{3a}$$

$$\begin{aligned}\widetilde{E}_{\alpha 3}^{so} &= \frac{1}{2}\left[\frac{\partial \mathbf{P}_I}{\partial \xi_\alpha}\frac{\partial\left(\overline{\mathbf{u}}_I + \xi_3\left(1-\frac{\xi_3^2}{3}\right)\overline{\mathbf{e}}_I\right)}{\partial \xi_3} + \frac{\partial \mathbf{u}_J}{\partial \xi_\alpha}\frac{\partial\left(\overline{\mathbf{P}}_I + \xi_3\left(1-\frac{\xi_3^2}{3}\right)\overline{\mathbf{V}}_J\right)}{\partial \xi_3}\right. \\ &\left. + \frac{\partial \mathbf{u}_K}{\partial \xi_\alpha}\frac{\partial\left(\overline{\mathbf{u}}_K + \xi_3\left(1-\frac{\xi_3^2}{3}\right)\overline{\mathbf{e}}_K\right)}{\partial \xi_3}\right] = \frac{1}{2}\left[\frac{\partial \mathbf{P}_I}{\partial \xi_\alpha}\overline{\mathbf{e}}_I + \frac{\partial \mathbf{u}_J}{\partial \xi_\alpha}\overline{\mathbf{V}}_J + \frac{\partial \mathbf{u}_K}{\partial \xi_\alpha}\overline{\mathbf{e}}_K\right]\left(1 - \xi_3^2\right)\end{aligned} \tag{3b}$$

If the ξ_3^2 term is excluded, the transverse natural shear strains in Eq. (3) are identical to those in the first-order shear deformation theory. Consequently, the combination of the transverse natural shear strains in the first-order shear deformation theory and Eq. (3) results in a parabolic through-thickness distribution for the transverse natural shear strains and satisfies the zero transverse shear stress requirement at the shell surfaces. Thus, it eliminates the need for the shear correction factors in the first-order theory. Finally, the ratio, h_ξ of effective transverse shear energy U_s to the average transverse shear energy $\overline{U}_s$ can be determined. In this paper, we present, in brief, the more general case of multilayer laminated composite plates where stresses are not continuous across the inter-lamina boundaries (Jung and Han 2014).

Equating two transverse shear strain energy expressions $(U_s = \overline{U}_s)$ and solving for the nominal uniform transverse shear strain $\overline{E}_{\alpha 3}$ give

$$\overline{E}_{\alpha 3} = \frac{\int \tilde{S}^s_{\alpha 3} \tilde{E}^s_{\alpha 3}\, d\xi_3}{\int \tilde{S}^s_{\alpha 3}\, d\xi_3} = \frac{\int H_\tau(\xi_3) H_\gamma(\xi_3)\, d\xi_3}{\int H_\tau(\xi_3)\, d\xi_3} \tilde{E}^e_{\alpha 3} \tag{4}$$

where $H_\tau(\xi_3)$ and $H_\gamma(\xi_3)$ are distribution shape function of transverse shear stress and strain, respectively. Therefore, the ratio of transverse shear strain effective magnitude $\tilde{E}^e_{\alpha 3}$ to the nominal uniform shear strain $\overline{E}_{\alpha 3}$ is

$$h_\xi = \frac{\tilde{E}^e_{\alpha 3}}{\overline{E}_{\alpha 3}} = \frac{\int H_\tau(\xi_3) d\xi_3}{\int H_\tau(\xi_3) H_\gamma(\xi_3) d\xi_3} \tag{5}$$

The modified first-order shear deformation theory can then be presented as a function of $(1 - x_3^2)$ and h_ξ factorizing the transverse shear strains in the first-order shear deformation theory as follows

$$\widetilde{E}^{sn}_{\alpha 3} = \widetilde{E}^{e}_{\alpha 3} \cdot H_\gamma(\xi_3) = \overline{E}_{\alpha 3} \cdot H_\gamma(\xi_3) \cdot h_\xi = \frac{1}{2}\left[\frac{\partial \mathbf{P}_I}{\partial \xi_\alpha}\overline{\mathbf{e}}_I + \frac{\partial \mathbf{u}_J}{\partial \xi_\alpha}\overline{\mathbf{V}}_J + \frac{\partial \mathbf{u}_K}{\partial \xi_\alpha}\overline{\mathbf{e}}_K\right]\left(1 - \xi_3^2\right) \cdot h_\xi \tag{6}$$

3. Various enhanced strain interpolation

The 8-node shell elements have been well documented in previous studies (Huang and Hinton 1986, Lakshinarayanan *et al*. 1989, MacNeal and Harder 1992, Bucalem and Bathe 1993, Kim and Park 2002, Kim *et al*. 2003). For the new modified 8-node non-linear shell element, the usual 8-nodes of two-dimensional quadratic serendipity displacement interpolations are employed and the various combinations of assumed natural strain interpolation functions are used. Fig. 2 illustrates

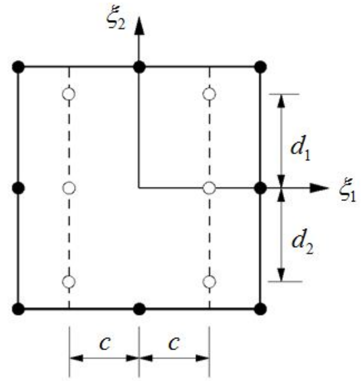

(a) Pattern α (following Bathe *et al*. (2003))

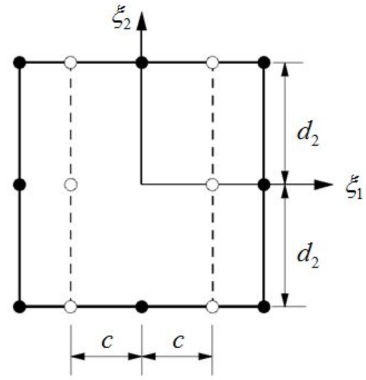

(b) Pattern β

Fig. 2 Five possible patterns of sampling points for 8-node ANS shell element

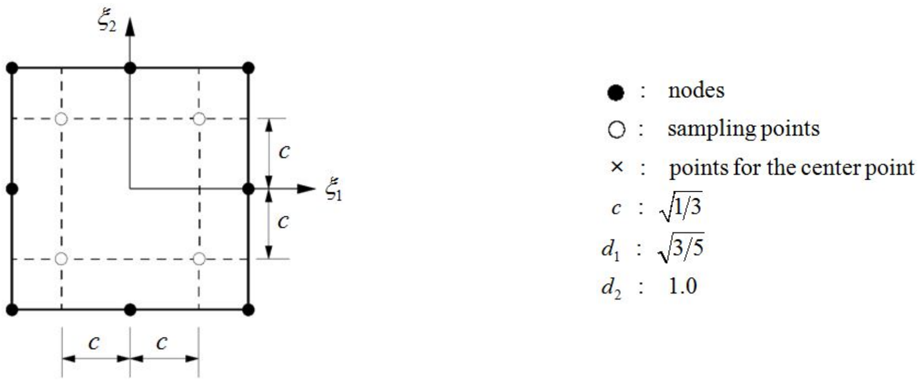

(c) Pattern δ

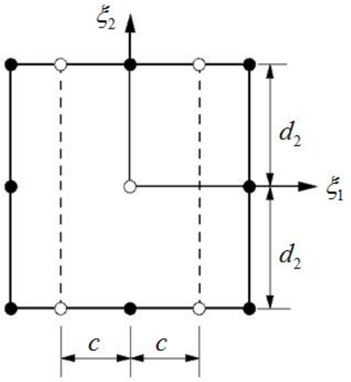

(d) Pattern γ (following Hwang (1989)

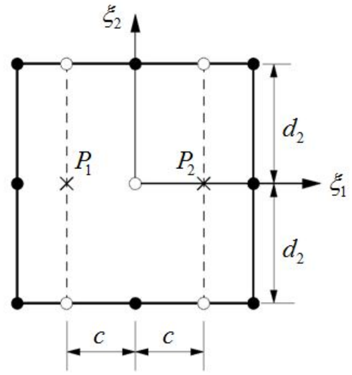

(e) Pattern γ_6, γ_6 (following Jung and Han (2013))

Fig. 2 Continued

various patterns of sampling points that can be employed for membrane, in-plane shear and transverse shear strain interpolations for the new 8-node shell element. The α pattern is used for membrane ($\alpha\delta\beta$ and $\alpha\delta\gamma$) and the β pattern is used for membrane ($\beta\delta\gamma$) as well as transverse shear ($\alpha\delta\beta$). The δ pattern and γ pattern are used for in-plane and transverse shear, respectively. The interpolation functions by Huang (1989) are used in the γ pattern.

The three cases of the combinations of various sampling points were used in Han *et al*. (2011) and the case ($\beta\delta\gamma_6^*$) were used in Jung and Han (2013). In this paper, based on the case proposed by Jung and Han (2013), the 8-nodes of the new combinations of assumed natural strain interpolation functions are used.

4. Strain energy and stress resultants of laminated shells

The stiffness properties are function of the normal coordinate in the laminated structures. A cross-section of laminated shell composed of N layers is presented in Fig. 3.

We introduce here an explicit transformation scheme between natural co-ordinates and the global co-ordinate system, to obtain a natural co-ordinate based constitutive equation, since the present formulation is based on the natural co-ordinate reference frame. (Kim and Park 2002,

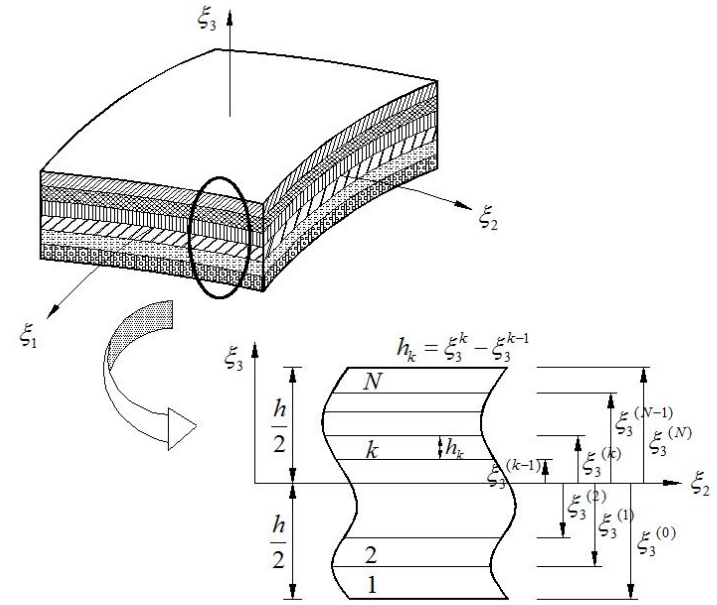

Fig. 3 Cross-section of laminated shell composed of N layers

Kim *et al*. 2003).

The stress tensor in the natural coordinate can be written as follows

$$\widetilde{S}_{ij} = \widetilde{C}_{ijkl}\widetilde{E}_{kl} = \widetilde{J}_0 \mathbf{T}\widetilde{D}_{ijkl}\mathbf{T}^{\mathbf{T}}\widetilde{E}_{kl} \tag{7}$$

where $\widetilde{C}_{ijkl}$ is the fourth order material tensor, $\widetilde{J}_0$ is the determinant of the Jacobian matrix and $\widetilde{D}_{ijkl}$ is the constitutive matrix for orthotropic materials with the material angle θ. The transformation matrix **T** in Eq. (7) is given by Han *et al*. (2004). The strain energy U can be expressed by

$$U = \frac{1}{2}\int_A \int_{-h/2}^{h/2} \widetilde{C}_{ijkl}\widetilde{E}_{ij}\widetilde{E}_{kl}\, d\xi_3\, dA \tag{8}$$

After integration, throughout the thickness, the strain energy can be obtained in terms of shell quantities: stress resultants and couples and laminated shell stiffness.

$$A^{(i)}_{\alpha\beta\gamma\delta} = \int_{-h/2}^{h/2} \widetilde{C}_{\alpha\beta\gamma\delta}\,(\xi_3^{(i)})\; d\xi_3\,, \qquad i = 0,1,2. \tag{9a}$$

$$A^{(i)}_{\alpha 3\beta 3} = \int_{-h/2}^{h/2} \widetilde{C}_{\alpha 3\beta 3}\,(\xi_3^{(i)})\; d\xi_3\,, \qquad i = 0,2,4. \tag{9b}$$

The shell element displays resultant forces acting on a laminate which are obtained by integration of stresses through the laminate thickness. The constitutive relations of the composite laminate are as follows

$$\begin{Bmatrix} M^{(0)}_{\alpha\beta} \\ M^{(1)}_{\alpha\beta} \end{Bmatrix} = \begin{bmatrix} A^{(0)}_{\alpha\beta\gamma\delta} & A^{(1)}_{\alpha\beta\gamma\delta} \\ A^{(1)}_{\alpha\beta\gamma\delta} & A^{(2)}_{\alpha\beta\gamma\delta} \end{bmatrix} \begin{Bmatrix} \tilde{E}^{m}_{\gamma\delta} \\ \tilde{E}^{b}_{\gamma\delta} \end{Bmatrix} \tag{10a}$$

$$\begin{Bmatrix} R^{(0)}_{\alpha 3} \\ R^{(1)}_{\alpha 3} \end{Bmatrix} = \begin{bmatrix} A^{(0)}_{\alpha 3\beta 3} & A^{(2)}_{\alpha 3\beta 3} \\ A^{(2)}_{\alpha 3\beta 3} & A^{(4)}_{\alpha 3\beta 3} \end{bmatrix} \begin{Bmatrix} \tilde{E}^{s1}_{\beta 3} \\ \tilde{E}^{s2}_{\beta 3} \end{Bmatrix} \tag{10b}$$

5. Equilibrium equation and tangent stiffness

When the static problems are considered, the equilibrium equation can be expressed as

$$\left(f_{j\beta}\tilde{S}_{\alpha\beta} \right)_{,\alpha} + \tilde{\rho} b_j = 0\,, \tag{11}$$

where $f_{j\beta}$ is the deformation gradient, $\tilde{S}_{\alpha\beta}$ is the second and symmetric natural stress tensor, $\tilde{\rho}$ is the mass density of the body, b_j is the body force and all these terms may be defined as

$$f_{j\beta} = \frac{\partial x_j}{\partial \xi_\beta},\;\; \tilde{S}_{\alpha\beta} = \tilde{J}_t \frac{\partial \xi_\alpha}{\partial x_i}\frac{\partial \xi_\beta}{\partial x_j}\sigma_{ij},\;\; \tilde{\rho} = \rho_0 \tilde{J}_t / J\,, \tag{12}$$

in which $\tilde{J}_t$ is $|\partial x_i/\partial \xi_\alpha|$, σ_{ij} is the Cauchy stress, ρ_0 is mass density of the undeformed body, and J is $|\partial P_I/\partial x_j|$.

The weak form can be constructed by Galerkin's weighted residual method as

$$G^e(\mathbf{u}, \delta\mathbf{u}) = -\int_{B^e} \left[\left(\tilde{S}_{\alpha\beta} f_{l\beta} \right)_{,\alpha} + \tilde{\rho} b_l \right] \delta u_l \, dV + \int_{\partial B^e} \left[\tilde{S}_{\alpha\beta} f_{l\beta} n_\alpha - T^{(N)}_l \right] \delta u_l \, dA = 0 \tag{13}$$

where $\mathbf{u}$ and $\delta\mathbf{u}$ are the displacement field and weight field, respectively; B^e and δB^e are the volume and its boundary surface of the parental element; and $T_l^{(N)}$ is a traction vector. Applying the Gauss-Green theorem, the above equation can be rewritten as

$$\int_{B^e} \tilde{S}_{\alpha\beta} f_{l\beta} \delta u_{l,\alpha} dV - \int_{B^e} \tilde{\rho} b_l \delta u_l \, dV - \int_{\partial B^e} T^{(N)}_l \, \delta u_l \, dA = 0 \tag{14}$$

The weight field of Galerkin's method can be expressed as

$$\delta\mathbf{u}(\xi_1, \xi_2, \xi_3) = \sum_{b=1}^{8} \frac{\partial \mathbf{x}(\xi_1, \xi_2, \xi_3)}{\partial \mathbf{U}^b} \delta\mathbf{U}^b = \sum_{b=1}^{8} \frac{\partial x_i(\xi_1, \xi_2, \xi_3)}{\partial U^b_j} \delta U^b_j \tag{15}$$

where $\delta\mathbf{U}^b$ denotes virtual nodal displacements. Substituting Eq. (15) into Eq. (14) yields

$$\begin{gathered} \int_{B^e} \tilde{S}_{\alpha\beta} f_{l\beta} \sum_{b=1}^{8} \frac{\partial}{\partial \xi_\alpha} \left(\frac{\partial x_l}{\partial \mathbf{U}^b} \right) \delta\mathbf{U}^b dV - \int_{B^e} \tilde{\rho} b_l \sum_{b=1}^{8} \left(\frac{\partial x_l}{\partial \mathbf{U}^b} \right) \delta\mathbf{U}^b dV - \int_{\partial B^e} T^{(N)}_l \sum_{b=1}^{8} \left(\frac{\partial x_l}{\partial \mathbf{U}^b} \right) \delta\mathbf{U}^b dA = 0 \\ \text{or} \;\; \sum_{b=1}^{8} \delta U^b_j \left(K^b_j - R^b_j \right) = 0 \end{gathered} \tag{16}$$

in which K_j^b is the internal force vector and R_j^b is the generalized force vector, respectively, defined as

$$K_j^b = \int_{B^e} \tilde{S}_{\alpha\beta} f_{l\beta} \frac{\partial}{\partial \xi_\alpha}\left(\frac{\partial x_l}{\partial U_j^b}\right) dV = \int_{B^e} \tilde{S}_{\alpha\beta} \frac{\partial x_l}{\partial \xi_\beta} \frac{\partial}{\partial \xi_\alpha}\left(\frac{\partial x_l}{\partial U_j^b}\right) dV,$$
$$R_j^b = \int_{B^e} \tilde{\rho} b_l \left(\frac{\partial x_l}{\partial U_j^b}\right) dV + \int_{\partial B^e} T_l^{(N)} \left(\frac{\partial x_l}{\partial U_j^b}\right) dA. \tag{17}$$

For the arbitrary variation of δU_j^b, Eq. (16) can be reduced as

$$K_j^b - R_j^b = 0 \qquad \text{or} \qquad \mathbf{K(U)} - \mathbf{R} = 0. \tag{18}$$

The linearization of internal force vector is required, and the result is the tangent stiffness in the form

$$\partial \mathbf{K}_{ji}^{ba} = \frac{\partial K_j^b}{\partial U_i^a} = \frac{\partial}{\partial U_i^a}\left(\int_{B^e} \tilde{S}_{\alpha\beta} \frac{\partial x_l}{\partial \xi_\beta} \frac{\partial}{\partial \xi_\alpha}\left(\frac{\partial x_l}{\partial U_j^b}\right) dV \right)$$
$$= \int_{B^e} \left[\frac{\partial x_l}{\partial \xi_\beta} \frac{\partial}{\partial \xi_\alpha}\left(\frac{\partial x_l}{\partial U_j^b}\right)\right] \tilde{C}_{\alpha\beta\gamma\delta} \left[\frac{\partial x_k}{\partial \xi_\delta} \frac{\partial}{\partial \xi_\gamma}\left(\frac{\partial x_k}{\partial U_i^a}\right)\right] dV \tag{19}$$
$$+ \int_{B^e} \left[\frac{\partial}{\partial \xi_\alpha}\left(\frac{\partial x_l}{\partial U_j^b}\right) \tilde{S}_{\alpha\beta} \frac{\partial}{\partial U_i^a}\left(\frac{\partial x_l}{\partial \xi_\beta}\right)\right] dV + \int_{B^e} \left[\tilde{S}_{\alpha\beta} \frac{\partial^2}{\partial U_i^a U_j^b}\left(\frac{\partial x_l}{\partial \xi_\alpha}\right)\left(\frac{\partial x_l}{\partial \xi_\beta}\right)\right] dV$$

In order to solve the nonlinear equation by the Newton-Raphson method, the linearization is required in the following form: (Kanok-Nukulchai *et al*. 1981)

$$\partial \mathbf{K}(\mathbf{U}_m^i) \Delta \mathbf{U}_m^i = \mathbf{R}_m - \mathbf{K}(\mathbf{U}_m^i) \tag{20}$$

where $\partial \mathbf{K}$ is the tangent stiffness with the value of a displacement $\mathbf{U}_m^i$ in which the subscript m refers to the current m^{th} load step and superscript i refers to the current i^{th} iteration step. The drilling degree of freedom will be linked to the in-plane twisting mode of the mid-surface by a penalty functional (Kanok-Nukulchai 1979).

6. Non-linear solution procedure

It is necessary to use the arc-length control method in order to trace the full path of load displacement, since the post-buckling study involves a highly distorted load-displacement path. With consideration of the incremental load step, Eq. (18) can be rewritten in the following form which has $(n + 1)$ unknowns

$$G(\mathbf{U}, \lambda) = \mathbf{K(U)} - \lambda \mathbf{F} = 0 \tag{21}$$

where $\mathbf{K(U)}$ is the internal force vector which is generally a non-linear function of $\mathbf{U}$ and $\mathbf{F}$ is a reference load vector. The non-linear equations are augmented by an additional constraint Eq. (22). (For more details, see Chaiomphob *et al*. 1998, Lee and Kanok-Nukulchai 1998)

$$f(\mathbf{U},\lambda)\ :\ \sum_{k=1}^{n}\chi_k\left(u_k^m-u_k^{m-1}\right)^2+\chi_{n+1}\alpha^2\left(\lambda^m-\lambda^{m-1}\right)^2=\sum_{k=1}^{n}\chi_k\Delta u_k^2+\chi_{n+1}\alpha^2\Delta\lambda^2=c^2 \tag{22}$$

where α denotes a load coefficient, c is the prescribed arc-length. For arc-length control method, $\sum_{k=1}^{n}\Delta u_k^2+\alpha^2\Delta\lambda^2=c^2$ when all $\chi_k = 1$.

Linearization of Eq. (21) and the constraint equation $f(\mathbf{U}, \lambda)$ with respect to $\mathbf{U}$ and λ about the previous solution ($\mathbf{U}^{i,m}$, $\lambda^{i,m}$) leads to the linearized equilibrium and constraint equation as follows

$$\partial\mathbf{K}^{i,m}\Delta\mathbf{U}^{i,m}-\mathbf{F}\Delta\lambda^{i,m}=\mathbf{R}^{i,m}=\lambda^{i,m}\mathbf{F}-\mathbf{K}(\mathbf{U}^{i,m}) \tag{23}$$

$$\begin{aligned}&2\sum_{i=1}^{n}\chi_k\left(\mathbf{U}^{i,m}-\mathbf{U}^{m-1}\right)\Delta\mathbf{U}^{i,m}+2\chi_{n+1}\alpha^2\left(\lambda^{i,m}-\lambda^{m-1}\right)\Delta\lambda^{i,m}\\&\qquad=c^2-\sum_{i=1}^{n}\chi_k\left(u_k^{i,m}-u_k^{m-1}\right)^2-\chi_{n+1}\alpha^2\left(\lambda^{i,m}-\lambda^{m-1}\right)^2\end{aligned} \tag{24}$$

where superscript ^{i,m} denotes the quantity at the ith iteration of the mth solution step, $\mathbf{R}^{i,m}$ is the unbalanced force vector and $\partial\mathbf{K}^{i,m}$ is the tangent stiffness matrix.

Finally, the non-linear equation augmented by a constraint equation can be written in matrix form

$$\begin{bmatrix}\partial\mathbf{K}^{i,m} & -\mathbf{F}\\ C_1^{\mathrm{T}} & C_2\end{bmatrix}\begin{Bmatrix}\Delta\mathbf{U}^{i,m}\\ \Delta\lambda^{i,m}\end{Bmatrix}=\begin{Bmatrix}\mathbf{R}^{i,m}\\ r^{i,m}\end{Bmatrix} \tag{25}$$

where $\partial\mathbf{K}^{i,m}$ is the tangent stiffness for a known displacement vector $\mathbf{U}^{i,m}$. If there is only solution step m in the superscript, that is $\mathbf{U}^m$, this is the final solution of the step m. The incremental quantities have the following relationship

$$\mathbf{U}^{i+1,m}=\mathbf{U}^{i,m}+\Delta\mathbf{U}^{i,m},\quad \lambda^{i+1,m}=\lambda^{i,m}+\Delta\lambda^{i,m} \tag{26}$$

7. Numerical examples

The present 8-node assumed strain shell element is implemented in the extended version of the FEAP (Zienkiewicz and Taylor 2000). In order to validate this present shell element, several numerical examples are solved to test the performance of the shell element in postbuckling analysis under shear loads. The results are presented in the non-dimensional form using Eq. (27)

$$\overline{P}=\frac{P\,a^2}{E_2h^3} \tag{27}$$

Fig. 4 shows the dimensions and coordinates of a laminated composite plate analyzed by the aforementioned theories for the materials whose properties are listed in Table 1. Fig. 5 also shows the loading types of a laminated composite plate. Full plate is analyzed with 8×8 mesh sizes.

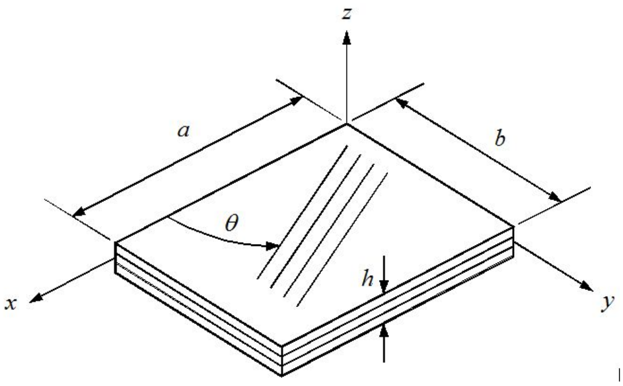

Fig. 4 Geometry of laminated composite plates ($a = b = 250$ mm, $h = 2.5$ mm)

Fig. 5 Positive and negative shear loading of a laminated composite plate: (a) Positive; (b) Negative

Table 1 Material properties (GPa)

Material	E_1	E_2	E_3	G_{12}	G_{23}	G_{13}	ν_{12}	ν_{23}	ν_{13}
Boron/Epoxy	206.9	20.7	20.7	5.2	5.2	5.2	0.3	0.3	0.3
Carbon/Epoxy	206.9	5.2	5.2	2.6	2.6	2.6	0.25	0.25	0.25
Glass/Epoxy	53.8	17.9	17.9	8.9	8.9	8.9	0.25	0.25	0.25

7.1 Validation

Firstly, the formulation with geometric nonlinearity is validated considering cross-ply [0°/90°/90°/0°] ($E_1/E_2 = 40$; $G_{12} = G_{13} = 0.6$; $G_{23} = 0.5$; $\nu_{12} = \nu_{23} = \nu_{13} = 0.25$) simply-supported thin (a/h = 100) square plates under in-plane positive shear loading (Balamurugan *et al*. 1998,

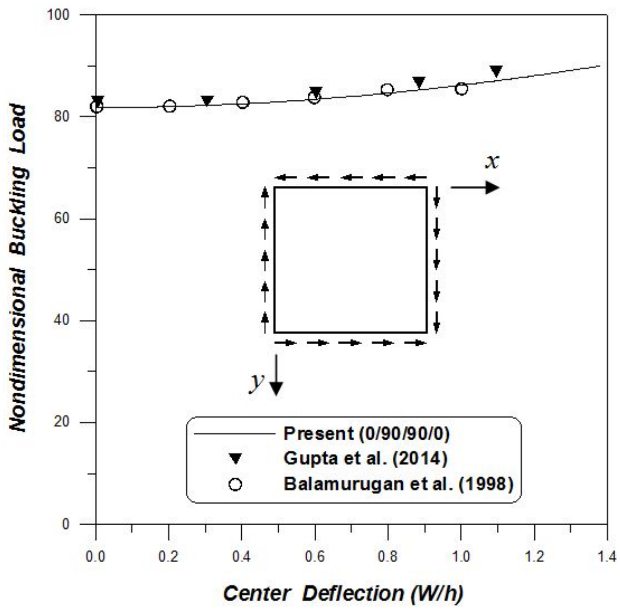

Fig. 6 Comparison of postbuckling response of simply supported laminated composite plate under positive shear loading

Gupta *et al*. 2014). The present results are found to be in excellent agreement with those of Balamurugan *et al*. (1998) and Gupta *et al*. (2014) as shown in Fig. 6.

Secondly, in order to show the effectivity of arc-length method the nonlinear analysis of cross-ply (0°/90°/0°) hinged shell is carried out with a 6.3 mm thickness (E_1 = 3.3 kN/mm^2, $E_2 = E_3$ = 1.1 kN/mm^2, $G_{12} = G_{13}$ = 0.6 kN/mm^2, G_{23} = 0.44 kN/mm^2, $v_{12} = v_{13} = v_{23}$ = 0.25). The geometry of shell is shown in Fig. 7 and the quarter model (3×3 meshes) is used.

To investigate the highly nonlinear behavior, arc-length control method is used. Based on this algorithm, the highly nonlinear equilibrium path is illustrated. The Fig. 8 shows the load-displacements curves for cross-ply hinged shell with a 6.3 mm thickness. Compared to the reference the present results are very good.

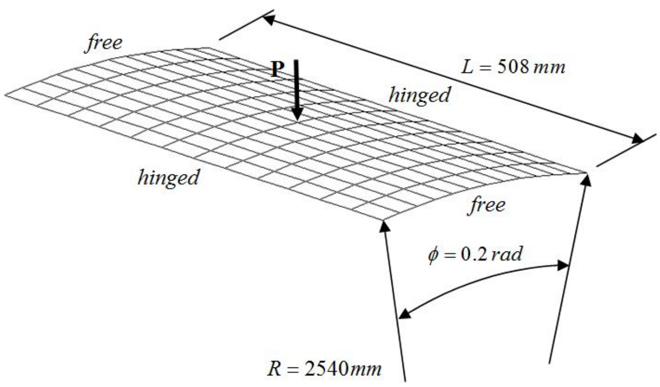

Fig. 7 Geometry of laminated composite hinged shell

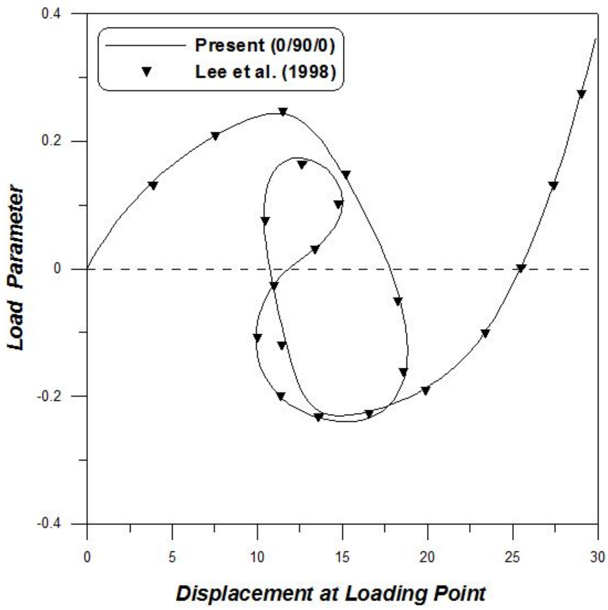

Fig. 8 Displacement of cylindrical laminated composite hinged shell under point load

7.2 Postbuckling response

A cylindrical shell with mid-surface radius R and thickness h, having length a and b, is shown in Fig. 9. The panel is assumed to consist of composite layer having different thickness, elastic properties and arbitrary orientations of orthotropic axes with respect to the generators of the panel. The panel is subjected to shear loading denoted by P_{xy} per unit length. The non-dimensional curvature parameter having the form

$$KR = \frac{a^2}{Rh} \tag{28}$$

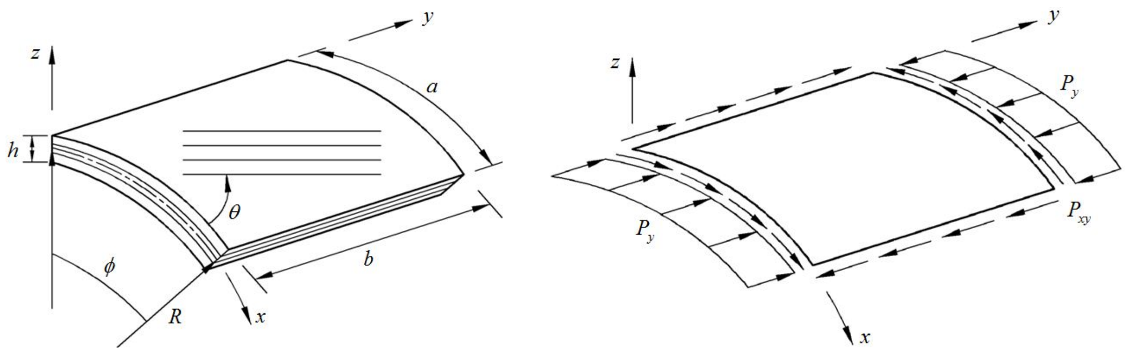

(a) Geometry of laminated composite shells (b) Negative shear loading of a laminated composite shell

Fig. 9 Geometry and positive shear loading of laminated composite shells ($a = b = 250$ mm, $h = 2.5$ mm)

The calculations refer to cylindrical shells with KR = 50 unless otherwise stated.

Figs. 10-17 represent the load-central deflection behavior of the curved panels after buckling. Fig. 8 shows the influence of lay-up on the postbuckling behavior of curved panels. The curves in the figure are obtained for boron/epoxy composites with the curvature parameter KR = 50. It may be seen that lay-up has a significant influence on the postbuckling behavior when the lay-up in the panel is symmetric. For panels with anti-symmetric lay-up the influence of the shear loadings seems more severe.

In Fig. 10, it is shown that the center deflection of symmetric laminated composite shells subjected to the pure shear loading for the different fiber angle. It may be noticed that the load-deflection curve of composite shells with the fiber angle of [–30°/30°/30°/–30°] exhibits the higher value than others by 4-15%.

Fig. 12 is for boron/epoxy laminated composite shells with symmetric and anti-symmetric angle-ply arrangements under the pure shear load. The results confirm the importance of the in-plane shear direction. Therefore it is important for designers to select correctly the fiber direction to obtain the higher performance of the laminated composite shells under the pure shear loading with prescribed load directions. Also, it can be observed that the alternate shear directions have no influence on the panel behavior for anti-symmetic angle-ply [–45°/45°/45°/–45°]. This is not difficult to understand because alternating shear direction is only equivalent to turning over the shell.

The effect of panel curvature on the load-deflection relations can be seen clearly from Fig. 13. Compared to the behavior of a flat plate, this means that a "jump" of the deflection may occur for curved panels when the shear load increases towards the bifurcation point. This kind of snap-through occurs in curved panels because there are more than one equilibrium states of the panels corresponding to a certain loading level. Because of without damage analysis it can be observed that the load-deflection curve of clamped plate goes beyond the generally possible deflection in

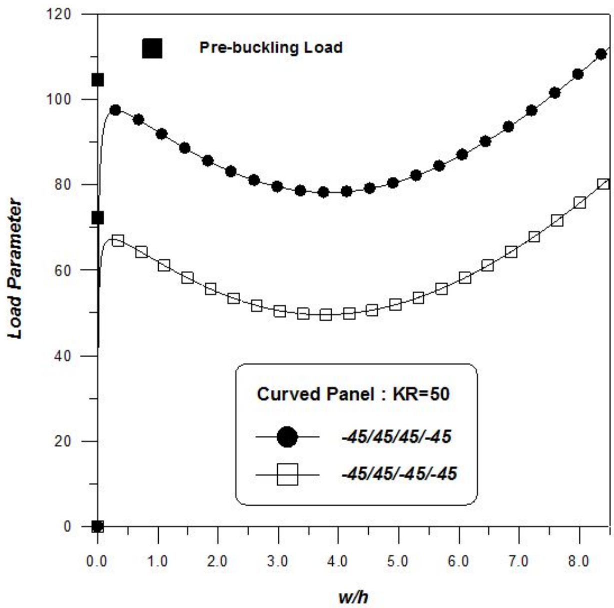

Fig. 10 Laminated composite curved panel with 2 lay-ups; Critical shear load, Boron/Epoxy, clamped edges

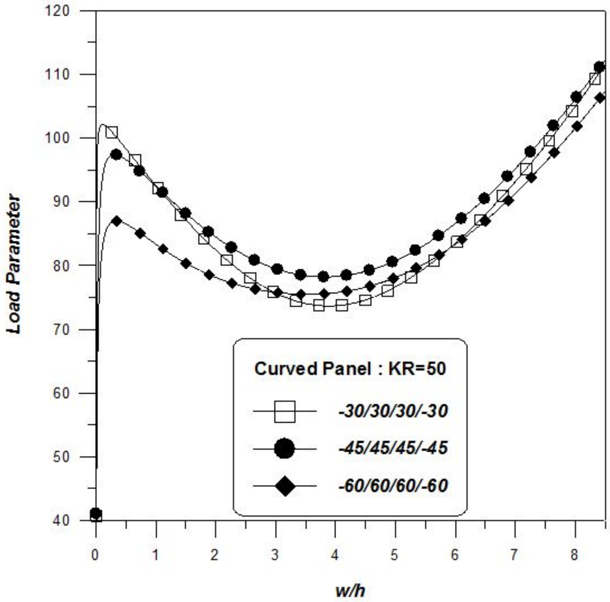

Fig. 11 Laminated composite curved panel with symmetric lay-ups; Critical shear load with fiber angle, Boron/Epoxy, clamped edges

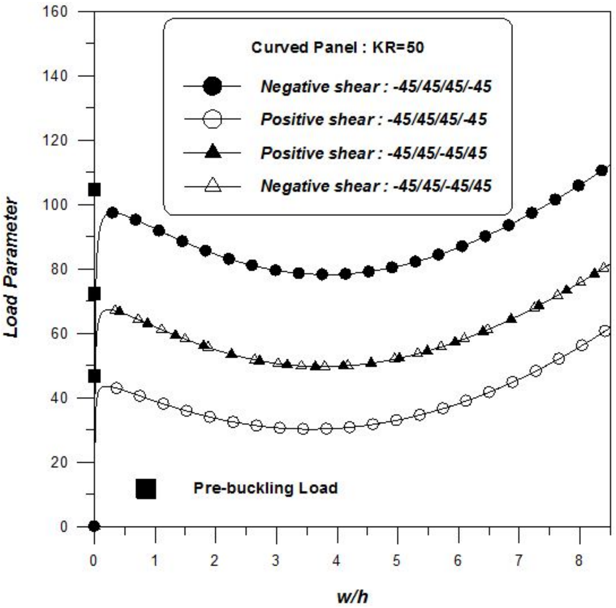

Fig. 12 Laminated composite curved panel with 2 lay-ups; Critical shear load with fiber angle, Boron/Epoxy, clamped edges

Fig. 13. It is noticed that further research work need to be focused on the damage or failureanalysis to improve the large deformation behavior of laminated composite structures.

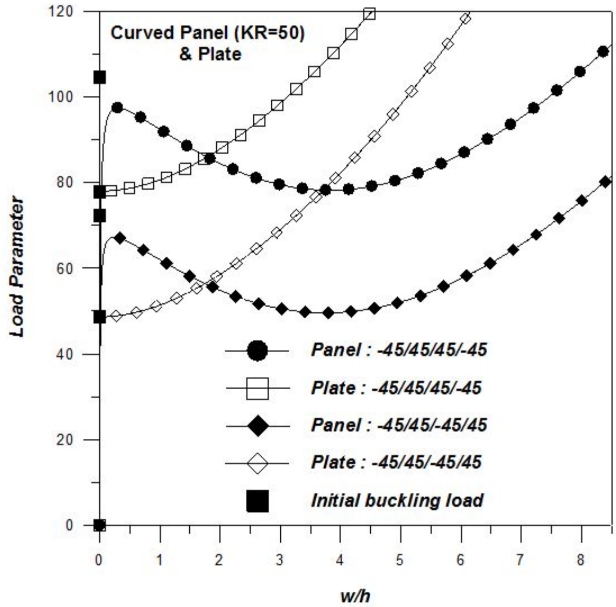

Fig. 13 Laminated composite plate and curved panel; Critical shear load, Boron/Epoxy, clamped edges

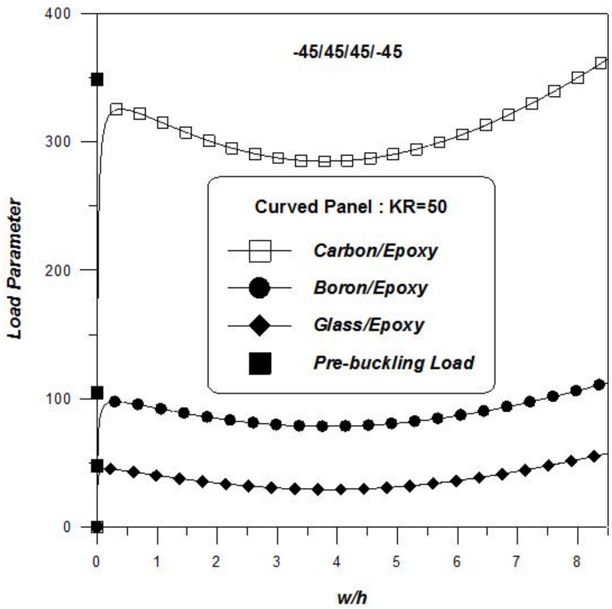

Fig. 14 Laminated composite curved panel; Critical shear load with material properties, clamped edges

Fig. 14 is for curved panels with $[m45°]_s$ lay-up and KR = 50. As expected, different materials have different postbuckling path. Fig. 13 refers to laminated composite shells having a $[m45°]_s$ lay-up of carbon/epoxy, boron/epoxy and glass/epoxy composite materials. The curves of deflection at the center of the shell versus the shear loading indicate that for the carbon/epoxy

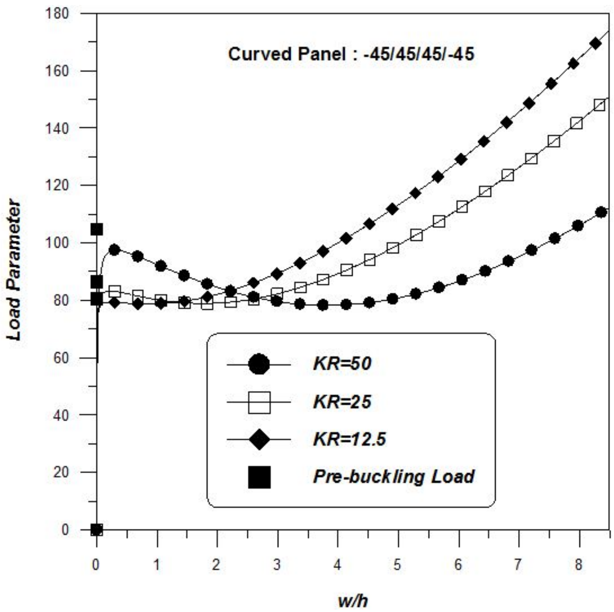

Fig. 15 Laminated composite curved panel; Critical shear load with radius, Boron/Epoxy, clamped edges

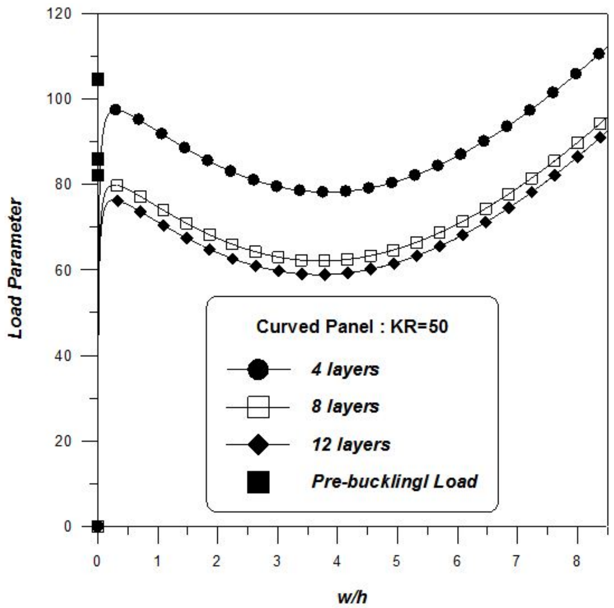

Fig. 16 Laminated composite curved panel; Critical shear load with layer numbers, Boron/Epoxy, clamped edges

shell, which has the higher ratio of E_1/E_2 for composite, the postbuckling path for negative shear direction is higher than for the boron/epoxy and glass/epoxy shells.

Fig. 15 shows the influence of laminated composite shell curvature. The figure is obtained for

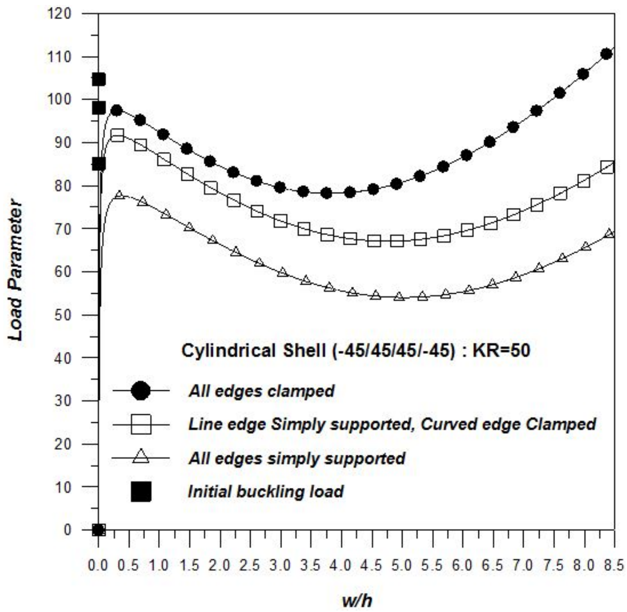

Fig. 17 Laminated composite shell with symmetric angle-ply lay-ups : negative shear loading; SS: all edges simply supported, SC: straight edge simply supported and curved edge clamped, CC: all edges clamped

four layer $[m45°]_s$ boron/epoxy panels. It is seen that the maximum snap-through load decreases when the panel becomes less curved and no snap-through load is found when the panel becomes very flat (say, $KR = 12.5$).

Fig. 16 is obtained for laminated composite boron/epoxy shells with symmetric angle-ply arrangements. The effect of increasing the number of alternate layers on the behavior of the shells under pure shear is demonstrated. It is observed that the number of layers have a significant effect on the buckling and post-buckling strength. The buckling and post-buckling strength decreases by increasing the number of layers. It is also observed that the number of layers beyond 8 does not have a significant effect. The load-central deflection curves indicate that for shells with such lay-ups, bending does not occur immediately in-plane shear loading is applied.

In Fig. 17, the influence of shear direction of symmetric angle-ply lay-up shells with different boundary conditions is presented. It is obtained for different boundary conditions. As expected, it is found that the buckling load-center deflection path of the cylindrical shell with all edges clamped is the highest for these three kinds of boundary conditions. All edges simply supported give the lowest buckling load-deflection path. These behaviors lead us to a conclusion that the influence of boundary conditions played a role in increasing or decreasing buckling load-deflection paths.

9. Conclusions

Postbuckling studies, even for laminated composite plates having special lay-ups under pure shear loading are few because of their complexity. The post-buckling response of a laminated composite plates and shells are obtained explicitly, using the modified 8-node ANS formulation with refined first-order shear deformation theory. Numerical results showing the effect of different loading, geometry, boundaries and lay-ups on the post-buckling response of the laminated composite plates and shells are obtained. The advanced finite element nonlinear analysis based on the modified 8-node ANS formulation shows the significance of stacking sequences and loading conditions for laminated composite shells. From the parametric case studies, a number of conclusions have been founded in designing laminated composite structures.

(1) The curvature of laminated composite shells has significant influence on the initial buckling and postbuckling behavior. For curved panels, the load-deflection become no longer monotonic and snap-through may occur when shear load becomes large. This is because there exist more than one equilibrium state of the panel corresponding to a certain shear loading level.
(2) The suitable selection of sampling points prevents the locking problem from occurring in buckling analysis of either thick panel or very thin panels.
(3) For initial buckling and postbuckling behavior of laminated composite shells, in-plane applied shear direction is a significant factor. For a constant shear loading, selecting the lay-up correctly to obtain the higher performance of the laminated composite shells is important.
(4) The lay-up arrangement in a laminated composite panel is also important for its initial buckling and postbuckling behavior. In symmetric case, increasing the number of alternate layers in the panel, while keeping the other conditions constant, gives lower performance of the panel.
(5) The postbuckling performance of a composite panel is affected by its boundary conditions. Clamped edges always produce a higher performance of the panel than simply supported edges.
(6) The postbuckling behavior of composite panels depends on the properties of the layers, in which the panel is composed. The properties of the materials do not change the trends of postbuckling behavior of the panels, although they do make a difference to the absolute values. Additionally, it is found that the effect of shear direction becomes more severe for a composite with a higher ratio of E_1 to E_2 than for one with a lower ratio.

To design the laminated composite shells under the in-plane shear loading, the present formulation and results may serve as benchmark for future guidelines and may be extended to dynamic instability, delamination, viscoelastic, damage, and failure analysis of various laminated composite structures. However, the parametric study proposed in this study is only an example and more studies should be carried out to apply the laminated composite shells for individual cases. The present study could be extended for finding post-buckling response of laminated composite plates and shells under mixed loading conditions. Also, the techniques should provide engineers with the capability for the design of composite structures including barrels, pipes, aircrafts, rockets, wing surfaces and missile skins.

Acknowledgments

This work was supported by the National Research Foundation of Korea [NRF] grant funded by the Korea Government [MEST] (No. 2011-0028531), and Basic Science Research Program through the National Research Foundation of Korea (NRF) funded by the Ministry of Education (2014R1A1A4A01008716).

References

Ait Amar Meziane, M., Abdelaziz, H.H. and Tounsi, A. (2014), "An efficient and simple refined theory for buckling and free vibration of exponentially graded sandwich plates under various boundary conditions", *J. Sandw. Struct. Mater.*, **16**(3), 293-318.

Ait Yahia, S., Ait Atmane, H., Houari, M.S.A. and Tounsi, A. (2015), "Wave propagation in functionally graded plates with porosities using various higher-order shear deformation plate theories", *Struct. Eng. Mech., Int. J.*, **53**(6), 1143-1165.

Bachir Bouiadjr, R., Bedia, E.A.A. and Tounsi, A. (2013), "Nonlinear thermal buckling behavior of functionally graded plates using an efficient sinusoidal shear deformation theory", *Struct. Eng. Mech., Int. J.*, **48**, 547-567.

Balamurugan, V., Ganapathi, M. and Patel, B.P. (1998), "Postbuckling behavior of anisotropic laminated composite plates due to shear loading", *Defense Sci. J.*, **48**(4), 433-440.

Bathe, K.J. and Dvorkin, E.N. (1986), "A formulation of general shell elements-The use of mixed interpolation of tensorial components", *Int. J. Numer. Method. Eng.*, **22**(3), 697-722.

Bathe, K.J., Lee, P.S. and Hiller, J.F. (2003), "Towards improving the MITC9 shell element", *Comput. Struct.*, **81**(8-11), 477-489.

Belabed, Z., Houari, M.S.A., Tounsi, A., Mahmoud, S.R. and Anwar Bég, O. (2014), "An efficient and simple higher order shear and normal deformation theory for functionally graded material (FGM) plates", *Compos.: Part B*, 60, 274-283.

Bennoun, M., Houari, M.S.A. and Tounsi, A. (2016), "A novel five variable refined plate theory for vibration analysis of functionally graded sandwich plates", *Mech. Adv. Mater. Struct.*, **23**(4), 423-431.

Bouderba, B., Houari, M.S.A. and Tounsi, A. (2013), "Thermomechanical bending response of FGM thick plates resting on Winkler-Pasternak elastic foundations", *Steel Compos. Struct., Int. j.*, **14**(1), 85-104.

Bourada, M., Kaci, A., Houari, M.S.A. and Tounsi, A. (2015), "A new simple shear and normal deformations theory for functionally graded beams", *Steel Compos. Struct., Int. J.*, **18**(2), 409-423.

Bousahla, A.A., Houari, M.S.A., Tounsi, A. and Adda Bedia, E.A. (2014), "A novel higher order shear and normal deformation theory based on neutral surface position for bending analysis of advanced composite plates", *Int. J. Comput. Method.*, **11**(6), 1350082.

Bucalem, M.L. and Bathe, K.J. (1993), "Higher-order MITC general shell elements", *Int. J. Numer. Method. Eng.*, **36**(21), 3729-3754.

Chaiomphob, T., Kanok-Nukulchai, W. and Nishino, F. (1998), "An automatic arc-length control algorithm for tracing equilibrium paths of nonlinear structures", *Struct. Eng. Earthq. Eng., JSCE*, **5**(1), 205-208.

Draiche, K., Tounsi, A. and Khalfi, Y. (2014), "A trigonometric four variable plate theory for free vibration of rectangular composite plates with patch mass", *Steel Compos. Struct., Int. J.*, **17**(1), 69-81.

Gupta, A.K., Patel, B.P. and Nath, Y. (2014), "Postbuckling response of composite laminated plates with evolving damage", *Int. J. Damage Mech.*, **23**, 222-244.

Hamidi, A., Houari, M.S.A., Mahmoud, S.R. and Tounsi, A. (2015), "A sinusoidal plate theory with 5-unknowns and stretching effect for thermomechanical bending of functionally graded sandwich plates", *Steel Compos. Struct., Int. J.*, **18**(1), 235-253.

Han, S.C., Kim, K.D. and Kanok-Nukulchai, W. (2004), "An element-based 9-node resultant shell element for large deformation analysis of laminated composite plates and shells", *Struct. Eng. Mech., Int. J.*, **18**(6), 807-829.

Han, S.C., Kanok-Nukulchai, W. and Park, W.T. (2011), "A refined finite element for first-order plate and shell analysis", *Struct. Eng. Mech., Int. J.*, **40**(2), 191-213.

Han, S.C., Park, W.T. and Jung, W.Y. (2015), "A four-variable refined plate theory for dynamic stability analysis of S-FGM plates based on physical neutral surface", *Compos. Struct.*, **131**, 1081-1089.

Hebali, H., Tounsi, A., Houari, M.S.A., Bessaim, A. and Bedia, E.A.A. (2014), "New quasi-3D hyperbolic shear deformation theory for the static and free vibration analysis of functionally graded plates", *J. Eng. Mech. (ASCE)*, **140**, 374-383.

Huang, H.C. (1989), *Static and Dynamic Analysis of Plates and Shells*, Springer-Verlag, London, UK.

Huang, H.C. and Hinton, E. (1986), “A new nine node degenerated shell element with enhanced membrane and shear interpolation”, *Int. J. Numer. Method Eng.*, **22**(1), 73-92.
Jones, R.M. (1973), “Buckling and vibration of unsymmetrically laminated cross-ply rectangular plates”, *AIAA*, **11**, 1626-1632.
Jung, W.Y. and Han, S.C. (2013), “An 8-node shell element for non-linear analysis of shells using the refined combination of membrane and shear interpolation functions”, *Math. Problem. Eng.*, **2013**, 1-16.
Jung, W.Y. and Han, S.C. (2014), “Shear buckling responses of laminated composite shells using a modified 8-node ANS shell element”, *Compos. Struct.*, **109**, 119-129.
Kanok-Nukulchai, W. (1979), “A simple and efficient finite element for general shell analysis”, *Int. J. Numer. Method Eng.*, **14**(2), 179-200.
Kanok-Nukulchai, W., Taylor, R.L. and Hughes, T.J.R. (1981), “A large deformation formulation for shell analysis by finite element method”, *Comput. Struct.*, **13**(1-3), 19-27.
Kim, K.D. and Park, T.H. (2002), “An 8-node assumed strain element with explicit integration for isotropic and laminated composite shells”, *Struct. Eng. Mech., Int. J.*, **13**(4), 1-18.
Kim, K.D., Lomboy, G.R. and Han, S.C. (2003), “A co-rotational 8-node assumed strain shell element for postbuckling analysis of laminated composite plates and shells”, *Computat. Mech.*, **30**(4), 330-342.
Kosteletos, S. (1992), “Shear buckling response of laminated plates”, *Compos. Struct.*, **20**, 147-154.
Kudva, N.J. (1979), “Postbuckling studies of curved laminated composite panels”, Ph.D. Thesis; Virginia Polytechnic Institute and State University, VA, USA.
Kumar, D. and Singh, S.B. (2010), “Postbuckling strengths of composite laminate with various shaped cutouts under in-plane shear”, *Compos. Struct.*, **92**(12), 2966-2978.
Lakshminarayana, H.V. and Kailash, K. (1989), “A shear deformable curved shell element of quadrilateral shape”, *Comput. Struct.*, **33**(4), 987-1001.
Lee, S.J. and Kanok-Nukulchai, W. (1998), “A nine-node assumed strain finite element for large-deformation analysis of laminated shells”, *Int. J. Numer. Method Eng.*, **42**(5), 777-798.
Ma, H. and Kanok-Nukulchai, W. (1989), “On the application of assumed strained methods”, *Proceedings of the Second East Asia-Pacific Conference on Structural Engineering and Construction*, Chiang Mai, Thailand, January.
MacNeal, R.H. and Harder, R.L. (1985), “A proposed standard set of problems to test finite element accuracy”, *Finite Elem. Anal. Des.*, **1**(1), 3-20.
MacNeal, R.H. and Harder, R.L. (1992), “Eight nodes or nine?”, *Int. J. Numer. Method. Eng.*, **33**(5), 1049-1058.
Mahi, A., Adda Bedia, E.A. and Tounsi, A. (2015), "A new hyperbolic shear deformation theory for bending and free vibration analysis of isotropic, functionally graded, sandwich and laminated composite plates”, *Appl. Math. Model.*, **39**, 2489-2508.
Reddy, J.N. (1984), “A simple higher order theory for laminated composite plates”, *J. Appl. Mech., ASME*, **51**, 745-752.
Tanov, R. and Tabiei, A. (2000), “Simple correction to the first-order shear deformation shell finite element formulations”, *Finite Elem. Anal. Des.*, **35**, 189-197.
Tounsi, A., Houari, M.S.A., Benyoucef, S. and Adda Bedia, E.A. (2013), A refined trigonometric shear deformation theory for thermoelastic bending of functionally graded sandwich plates”, *Aerosp. Sci. Technol.*, **24**, 209-220.
Vinson, J.R. and Chou, T.W. (1975), *Composite Materials and their Use in Structures*, Applied Science Publishers Ltd., London, UK.
Whitney, J.M. (1969a), “Bending-extensional coupling in laminated plates under transverse loading”, *J. Compos. Mater.*, **3**, 20-28.
Whitney, J.M. (1969b), “The effect of transverse shear deformation on the bending of laminated plates”, *J. Compos. Mater.*, **3**, 534-547.
Wilkins, D.J. and Olson, F. (1974), “Shear buckling of advanced composite curved panels”, *J. Experim. Mech.*, **14**(8), 326-330.
Zhang, Y. and Matthews, F.L. (1983a), “Initial buckling of curved panels of generally layered composite

materials", *Compos. Struct.*, **1**, 3-30.
Zhang, Y. and Matthews, F.L. (1983b), "Postbuckling behaviour of curved panels of generally layered composite materials", *Compos. Struct.*, **1**, 115-135.
Zhang, Y. and Matthews, F.L. (1985), "Large deflection behavior of simply supported laminated panels under in-plane loading", *J. Appl. Mech., ASME*, **52**(3), 553-558.
Zidi, M., Tounsi, A., Houari, M.S.A., Adda Bedia, E.A. and Anwar Bég, O. (2014), "Bending analysis of FGM plates under hygro-thermo-mechanical loading using a four variable refined plate theory", *Aerosp. Sci. Technol.*, **34**, 24-34.
Zienkiewicz, O.C. and Taylor, R.L. (2000), *The Finite Element Method*, Butterworth-Heinemann, London, UK.

CC